NEOPLASIA
www.neoplasia.com

Volume 12 Number 3 March 2010 pp. 235–243 235

Dual Loss of *Rb1* and *Trp53* in the Adrenal Medulla Leads to Spontaneous Pheochromocytoma[1]

Ian D. Tonks*, Arne W. Mould*, Wayne A. Schroder*, Andrew Cotterill†, Nicholas K. Hayward*, Graeme J. Walker* and Graham F. Kay*

*Queensland Institute of Medical Research, Herston, Queensland, Australia; †Department of Endocrinology and Diabetes, Mater Children's Hospital, Brisbane, Queensland, Australia

Abstract

Using a Cre/loxP system, we have determined the phenotypic consequences attributable to *in vivo* deletion of both *Rb1* and *Trp53* in the mouse adrenal medulla. The coablation of these two tumor suppressor genes during embryogenesis did not disrupt adrenal gland development but resulted in the neoplastic transformation of the neural crest–derived adrenal medulla, yielding pheochromocytomas (PCCs) that developed with complete penetrance and were inevitably bilateral. Despite their typically benign status, these PCCs had profound ramifications on mouse vitality, with effected mice having a median survival of only 121 days. Evaluation of these PCCs by both immunohistochemistry and electron microscopy revealed that most $Rb1^{-/-}$:$Trp53^{-/-}$ chromaffin cells possessed atypical chromagenic vesicles that did not seem capable of appropriately storing synthesized catecholamines. The structural remodeling of the heart in mice harboring $Rb1^{-/-}$:$Trp53^{-/-}$ PCCs suggests that the mortality of these mice may be attributable to the inappropriate release of catecholamines from the mutated adrenal chromaffin cells. On the basis of the collective data from *Rb1* and *Trp53* knockout mouse models, it seems that the conversion of *Rb1* loss–driven adrenal medulla hyperplasia to PCC can be greatly enhanced by the compound loss of Trp53, whereas the loss of Trp53 alone is generally ineffectual on adrenal chromaffin cell homeostasis. Consequently, the *Trp53* tumor suppressor gene is an efficient genetic modifier of *Rb1* loss in the development of PCC, and their compound loss in the adrenal medulla has a profound impact on both cellular homeostasis and animal vitality.

Neoplasia (2010) 12, 235–243

Introduction

Development and cellular homeostasis necessitates the orchestrated interplay of oncogene and tumor suppressor gene functions. Disruption of this delicate interaction can lead to transformation, and an integral event in this process is the escape of the cell cycle from normal regulatory constraints.

The cell cycle is driven by the activity of the cyclin-dependent kinase (Cdk)–cyclin complexes that phosphorylate and modify target proteins to facilitate cell cycle progression. Consequently, the maintenance of cellular homeostasis dictates that Cdk-cyclin function is stringently regulated. This occurs by a number of diverse mechanisms ranging from the regulation of cyclin expression levels through to the activity of the cyclin-dependent kinase inhibitors (CKIs), which are divided into two subfamilies based on their substrate specificity. The Ink4 CKIs (p15, p16, p18, and p19) inhibit Cdk4/6–cyclin D complexes, whereas the less specific Cip1/Kip1 inhibitors (p21, p27, and p57) bind a number of different Cdk-cyclins but only inhibit specific combinations [1,2]. These different classes of CKIs act synergistically to suppress cell cycle progression by inhibiting Cdk-cyclin function [3,4].

The perturbation of Cdk-cyclin function seems to be essential in pheochromocytoma (PCC), a catecholamine producing tumor derived from the chromaffin cells of the adrenal medulla. Indeed, p16, p18,

Abbreviations: Cdk, cyclin-dependent kinase; CKI, cyclin-dependent kinase inhibitor; floxed, loxP flanked; PCC, pheochromocytoma; PP, pocket protein; TEC, tyrosinase-expressing Cre

Address all correspondence to: Dr. Ian Tonks, Queensland Institute of Medical Research, Herston, Queensland, Australia. E-mail: Ian.Tonks@qimr.edu.au

[1]This work was supported by a grant from the Cancer Council Queensland (442956). N.K.H. and G.F.K. are supported by fellowships from the National Health and Medical Research Council of Australia and the Cancer Council Queensland, respectively.
Received 23 September 2009; Revised 23 December 2009; Accepted 29 December 2009

DOI 10.1593/neo.91646

and p27 CKIs have all been identified as tumor suppressors relevant to this tumor type [5–7]. Furthermore, overexpression of cyclin D or cyclin E has also been identified as having an oncogenic function in PCC [6,8].

Some of the primary targets of Cdk-cyclins in cell cycle progression are the pocket proteins (PPs), Rb1 (retinoblastoma), retinoblastoma-like 1 (Rbl1, also known as p107), and retinoblastoma-like 2 (Rbl2, also known as p130). The PPs constitute an important family of tumor suppressors that regulate cell cycle progression. Although all PPs have tumor suppressive function, the strength of this function varies for each member of the family. Rb1 is generally regarded as having the strongest tumor suppressive activity and, whereas both *Rbl1* and *Rbl2* alone are competent in this regard [9–11], they seem to function most strongly in synergy with *Rb1* [12,13]. The PPs are also key players in tissue development, with cell autonomous and nonautonomous roles in homeostasis [14]. Despite their functional redundancy, the interactions of the PPs are complex because different members can fulfill diametrically opposed functions during development, as typified in adipose tissue and skeletal muscle [15–17].

In mice younger than 6 months, *Rb1* loss contributes significantly to adrenal cell hyperplasia, which is an intermediate step to PCC, although PCC can be observed in older $Rb1^{+/-}$ mice [18,19]. In this context, the transition from hyperplasia to PCC is seen to have occurred when the hyperplastic cells occupy greater than 50% of the adrenal volume and they have started to either compress or invade the cortex [20]. In humans, *Rb1* loss is relatively common in PCC but is an early event in the tumorigenic cascade, requiring further genetic modifications to facilitate neoplastic transformation of hyperplastic cells [21]. It is known from murine models that the loss of *Rbl2*, but not *Rbl1*, may serve as an important modifier of *Rb1* [22]. In this study, we show that the *Trp53* tumor suppressor gene is also an efficient genetic modifier of *Rb1* loss in the development of PCC.

Materials and Methods

Mice, Genotyping, and Strain Considerations

All mice were treated in accordance with the Australian Government National Health and Medical Research Council guidelines for the care of experimental animals. The derivation of $Rb1^{F2/F2}$, *TEC1*, and $Trp53^{F2\text{-}10/F2\text{-}10}$ mice has been described elsewhere [23–25]. To mediate deletion of loxP flanked (floxed) *Rb1* ($Rb1^{F2/F2}$) [23] and *Trp53* ($Trp53^{F2\text{-}10/F2\text{-}10}$) alleles [25], *Cre* recombinase expression was driven from the *TEC1* transgene by using *Tyrosinase* (*Tyr*) transcriptional elements [24]. The *Tyr* transcriptional elements are, or were, active in the development in a subset of neural crest–derived tissues including the adrenal medulla, melanocytes, and Schwann cells of the peripheral nervous system, and this will target the loss of the floxed *Rb1* and *Trp53* alleles specifically to these tissues [24]. Polymerase chain reaction (PCR) detection of the wild type, floxed, and deleted alleles used Rb5/(5′-acctagcctgagagtaggcaac-3′)/$Rb_{amp3\text{-}2}$ (5′-catctacagcaggtagatgccc-3′) and T008/T009/T011 primers for *Rb1* [23] and *Trp53* [25], respectively.

The genetic backgrounds of the mice used to breed $Rb1^{F2/F2}$:$Trp53^{F2\text{-}10/F2\text{-}10}$:*TEC1*, $Rb1^{F2/+}$:$Trp53^{F2\text{-}10/F2\text{-}10}$:*TEC1*, and $Rb1^{F2/F2}$:$Trp53^{F2\text{-}10/F2\text{-}10}$ cohorts were as follows: the *TEC1* transgenic mice were backcrossed for 20 generations with C57BL/6J; the 129/SV:C57BL/6J crossbred $Rb1^{F2/F2}$ mice were backcrossed for a minimum of two generations with C57BL6/J before use. The $Trp53^{F2\text{-}10/F2\text{-}10}$ mice were obtained from the National Institutes of Health mouse repository and were on a FVB:129 background. Consequently, resultant mice from the breeding program were a mixed C57BL/6J:FVB:129/SV background.

Tissue Culture

The medulla of $Rb1^{F2/F2}$:$Trp53^{F2\text{-}10/F2\text{-}10}$:*TEC1* and $Rb1^{F2/F2}$:$Trp53^{F2\text{-}10/F2\text{-}10}$ adrenal glands were physically decapsulated from the cortex, minced, and enzymatically dissociated with trypsin. The dissociated chromaffin cells were subsequently cultured in Dulbecco's modified Eagle medium (Invitrogen, Carlsbad, CA), 10% FBS, 2 mM L-glutamine, 100 U of penicillin, 100 μg of streptomycin, and 100 μM nonessential amino acids.

Tissue Preparation and Immunohistochemistry

The Cre-expressing tissues including the adrenal glands and skin, as well as a number of other tissues, including the heart, were dissected from mice of appropriate genotype, washed in PBS, and then fixed overnight at 4°C in 4% paraformaldehyde (Sigma, St Louis, MO) in PBS. Samples were subsequently washed in PBS three times for 15 minutes per wash, placed in 70% ethanol, and prepared for paraffin blocks. Before paraffin blocking, the hearts were cut perpendicular to their long axis at a point from their base equivalent to two-thirds of their overall length. All tissue samples were paraffin-blocked, and 4-μm sections were subsequently cut onto SuperFrost plus slides (HD Scientific, Wetherill Park, NSW, Australia). For histologic analysis, the slides from the adrenal glands and heart were subjected to standard hematoxylin and eosin (H&E; HD Scientific) staining followed by coverslipping.

To detect cellular proliferation, immunohistochemistry was performed with antibodies against both MCM7 and Ki67, which detect cellular proliferation. Tyrosine hydroxlase immunohistochemistry was used to determine whether catecholamine synthetic pathways were active in cells whereas antibodies against chromogranin A and synaptophysin were used to determine the integrity of chromagenic vessels that store catecholamines.

For MCM7, Ki67, tyrosine hydroxylase, chromogranin A, and synaptophysin immunohistochemistry, the adrenal gland sections were dewaxed in xylene (Ajax, Sydney, Australia) and rinsed in PBS, and citrate retrieval of the antigen was performed in a pressure cooker using 10 mM citrate buffer (1.47 g of trisodium citrate dihydrate [Ajax] dissolved in 1 L of distilled water and adjusted to pH 6.0 with 1 M sodium hydroxide [Ajax]) by heating the slides to 125°C for 15 minutes followed by 10 seconds at 90°C. The sections were subsequently left to cool to ambient temperature and rinsed with PBS. Endogenous peroxidase activity in sections used for MCM7, tyrosine hydroxylase, chromogranin A, and synaptophysin immunohistochemistry was neutralized using 3% H_2O_2/1% NaN_3 (Sigma) in PBS for 30 minutes at 25°C.

Slides were rinsed in PBS twice, washed for a further 3 minutes, and incubated in 10% goat serum (diluted in PBS) for 30 minutes at 25°C. The serum block was removed, and a 1:200 dilution of either rabbit anti–chromogranin A (Zymed, South San Francisco, CA), rabbit anti–tyrosine hydroxylase (Chemicon, Temacula, CA), or rabbit anti-MCM7 antibody (Abcam, Cambridge, UK) in PBS was added and the slides were incubated overnight at 4°C. In the case of synaptophysin immunohistochemistry after the goat serum block, the slides were washed three times in PBS for 5 minutes per wash, overlaid with a 1:200 dilution of goat antimouse immunoglobulin class G (Jackson ImmunoResearch Laboratories, West Grove, PA) in PBS for 30 minutes followed by three washes in PBS for 5 minutes per wash.

A 1:4 dilution of the mouse monoclonal anti–synapthophysin antibody (SY38; Abcam) was added, and the slides were slides incubated overnight at 4°C.

At the completion of the overnight incubation, the slides were then rinsed in PBS twice and washed for a further 3 minutes, and Dako anti–Rabbit envision (Dako, Glostrup, Denmark) was added to the MCM7, tyrosine hydroxylase, and chromogranin A slides, whereas Dako antimouse envision (Dako) was used for the synaptophysin slides. After a 30-minute incubation at 25°C, the slides were washed quickly three times in PBS, given a final 5-minute wash, and were immersed in DAB to develop color (2-10 minutes; the reaction was terminated when the positive control included for each sample gave obvious color development.). At the completion of incubation, slides were rinsed in distilled water, counterstained with hematoxylin (HD Scientific), washed in tap water, dehydrated, and coverslipped.

In the case of Ki67 (Dako), immunohistochemistry of the sectioned adrenal glands was performed as described elsewhere [26].

Electron Microscopy

Electron microscopy of chromaffin cells obtained from $Rb1^{F2/F2}$:$Trp53^{F2\text{-}10/F2\text{-}10}$:*TEC1* and $Rb1^{F2/F2}$:$Trp53^{F2\text{-}10/F2\text{-}10}$ mice was performed as described elsewhere [27].

Glyoxylic Acid Condensation Reaction

Adrenal glands from $Rb1^{F2/F2}$:$Trp53^{F2\text{-}10/F2\text{-}10}$:*TEC1* and $Rb1^{F2/F2}$:$Trp53^{F2\text{-}10/F2\text{-}10}$ mice were harvested, washed in PBS, and blocked in optimal cutting temperature compound (Tissue Tek, Tokyo, Japan). Glyoxylic acid condensation reactions, to detect biogenic amines, were performed on 7-μm sections of these adrenal glands using the protocol described by De la Torre [28].

Results

The Loss of Rb1 and Trp53 in Tyr-Expressing Tissues In Vivo *Leads to Adrenal Medulla Tumors*

We have been interested in the role of the PP and Trp53 regulatory axis in maintaining the homeostasis of the neural crest–derived tissues. To this end, we have been using floxed Rb1 ($Rb1^{F2/F2}$) [23] and Trp53 ($Trp53^{F2\text{-}10/F2\text{-}10}$) [25] mice crossed with $TEC1^{+/-}$ (tyrosinase-expressing Cre) transgenic mice to drive Cre recombinase expression and ablation of these floxed alleles in *Tyrosinase* transcriptional domains. This yields a tissue-specific knockout in neural crest–derived tissues that actively express *Tyrosinase* or have done so at any given stage in their development, in this case the adrenal medulla, melanocytes, and Schwann cells of the peripheral nervous system [24]. To examine the cell autonomous effects of *Rb1* and *Trp53* loss in these tissues, cohorts of $Rb1^{F2/F2}$:$Trp53^{F2\text{-}10/F2\text{-}10}$:$TEC1^{+/-}$, $Rb1^{F2/+}$:$Trp53^{F2\text{-}10/F2\text{-}10}$:$TEC1^{+/-}$, and floxed control animals (n = 13 for each group) were bred at the expected Mendelian ratios from the parental strains and were phenotypically examined over an 8-month time frame. Within this study, all floxed control animals remained viable and healthy. Of the 13 mice from the $Rb1^{F2/+}$:$Trp53^{F2\text{-}10/F2\text{-}10}$:$TEC1^{+/-}$ cohort, 2 did not survive the time course. One of these animals required euthanasia owing to a seemingly unrelated problem (bowel blockage), and we were unable to determine the cause of death underpinning the other mortality. In contrast, none of the $Rb1^{F2/F2}$:$Trp53^{F2\text{-}10/F2\text{-}10}$:$TEC1^{+/-}$ animals survived beyond 8 months, with the median survival time being 121 days (Figure 1*A*).

The mortality of the $Rb1^{F2/F2}$:$Trp53^{F2\text{-}10/F2\text{-}10}$:$TEC1^{+/-}$ animals was not due to melanocytic lesions because none of the cohort showed pigmentation defects or melanoma, although the melanocytes were *Rb1* and *Trp53*-null [29]. This was surprising because the PPs and Trp53/Mdm2/Arf regulatory axes are presumed to fulfill an integral role in melanocyte homeostasis. It was also significant that within the $Rb1^{F2/F2}$:$Trp53^{F2\text{-}10/F2\text{-}10}$:$TEC1^{+/-}$ cohort, 10 of the 13 mice appeared asymptomatic before death. They had no obvious external macroscopic masses, distal metastasis, or wasting, and there was no obvious physical predictor of impending death. Consequently, when necroscopy was performed, particular attention was paid to whether perturbations existed in the remaining Cre recombinase expressing tissues (i.e., the adrenal medulla or peripheral nervous system). In this context, it was observed that all of the $Rb1^{F2/F2}$:$Trp53^{F2\text{-}10/F2\text{-}10}$:$TEC1^{+/-}$ mice had enlarged adrenal glands compared with $Rb1^{F2/+}$:$Trp53^{F2\text{-}10/F2\text{-}10}$:$TEC1^{+/-}$ and $Rb1^{F2/F2}$:$Trp53^{F2\text{-}10/F2\text{-}10}$ control animals (Figure 1, *B* and *C*) and this was invariably bilateral. The enlarged adrenal glands remained encapsulated by the cortex and did not interdigitate into or invade surrounding tissues, and consistent with the aforementioned absence of external distal metastasis, no other gross lesions were apparent in other internal tissues examined.

The remaining $Rb1^{F2/F2}$:$Trp53^{F2\text{-}10/F2\text{-}10}$:$TEC1^{+/-}$ mice also possessed bilateral enlarged adrenal glands but, in contrast to the remainder of the cohort, they also displayed wasting, and tumor masses were present in regions remote from the adrenal gland. In two of these cases, the locality of the tumor masses was consistent with the trigeminal nerve–derived schwannomas described for $Prkra1^{F/F}$:*TEC3* mice [30] (data not shown). The third case seemed an exception to the rest of the cohort because it possessed a tumor mass localized to the neck region, which may have represented a distal metastasis from the adrenal glands.

Because the only overt defect in most $Rb1^{F2/F2}$:$Trp53^{F2\text{-}10/F2\text{-}10}$:$TEC1^{+/-}$ mice was the adrenal glands, this tissue was subjected to further characterization. The histologic analysis of $Rb1^{F2/F2}$:$Trp53^{F2\text{-}10/F2\text{-}10}$ adrenal glands indicated that the chromaffin cells all had nuclei of consistent size and shape (Figure 1*D*). In contrast, at time points as early as 56 days postpartum, the $Rb1^{F2/F2}$:$Trp53^{F2\text{-}10/F2\text{-}10}$:*TEC1* medulla showed distinct foci or clusters of cells with atypical H&E staining and aberrant nuclear morphology (Figure 1*E*). They possessed highly variable nuclear shape and volume, ranging from smaller irregularly shaped nuclei through to large polymorphic nuclear aggregates (Figure 1*F*). This is similar to cultured $Rb1^{F2/F2}$:$Trp53^{F2\text{-}10/F2\text{-}10}$:*TEC1* melanocytes, where the loss of *Rb1* and *Trp53* causes cells to rapidly become hypoploid and hyperploid owing to defects in mitosis, such as multipolar mitosis and cytokinesis [29].

This suggests that the mice initially develop hyperplastic foci of adrenal medulla chromaffin cells that rapidly progress to PCC by 112 days because the entire volume of the medulla was occupied by these atypical cells, and the cortex was significantly compressed (Figure 1*G*). The overall tissue architecture of the $Rb1^{F2/F2}$:$Trp53^{F2\text{-}10/F2\text{-}10}$:*TEC1* adrenal medullas also seem typical for PCC, being heterogeneous with both the expected zellballan and trabeculae configurations being noted (data not shown). The highly proliferative status of $Rb1^{F2/F2}$:$Trp53^{F2\text{-}10/F2\text{-}10}$:*TEC1* chromaffin cells was illustrated by the expression of the proliferation marker Ki67 (Figure 1*H*), which was absent in controls (Figure 1*I*). An identical result was also obtained with another proliferative marker, MCM7 (data not shown).

To confirm that the chromaffin cells from $Rb1^{F2/F2}$:$Trp53^{F2\text{-}10/F2\text{-}10}$:*TEC1* mice were *Rb1* and *Trp53* null, they were cultured and subjected

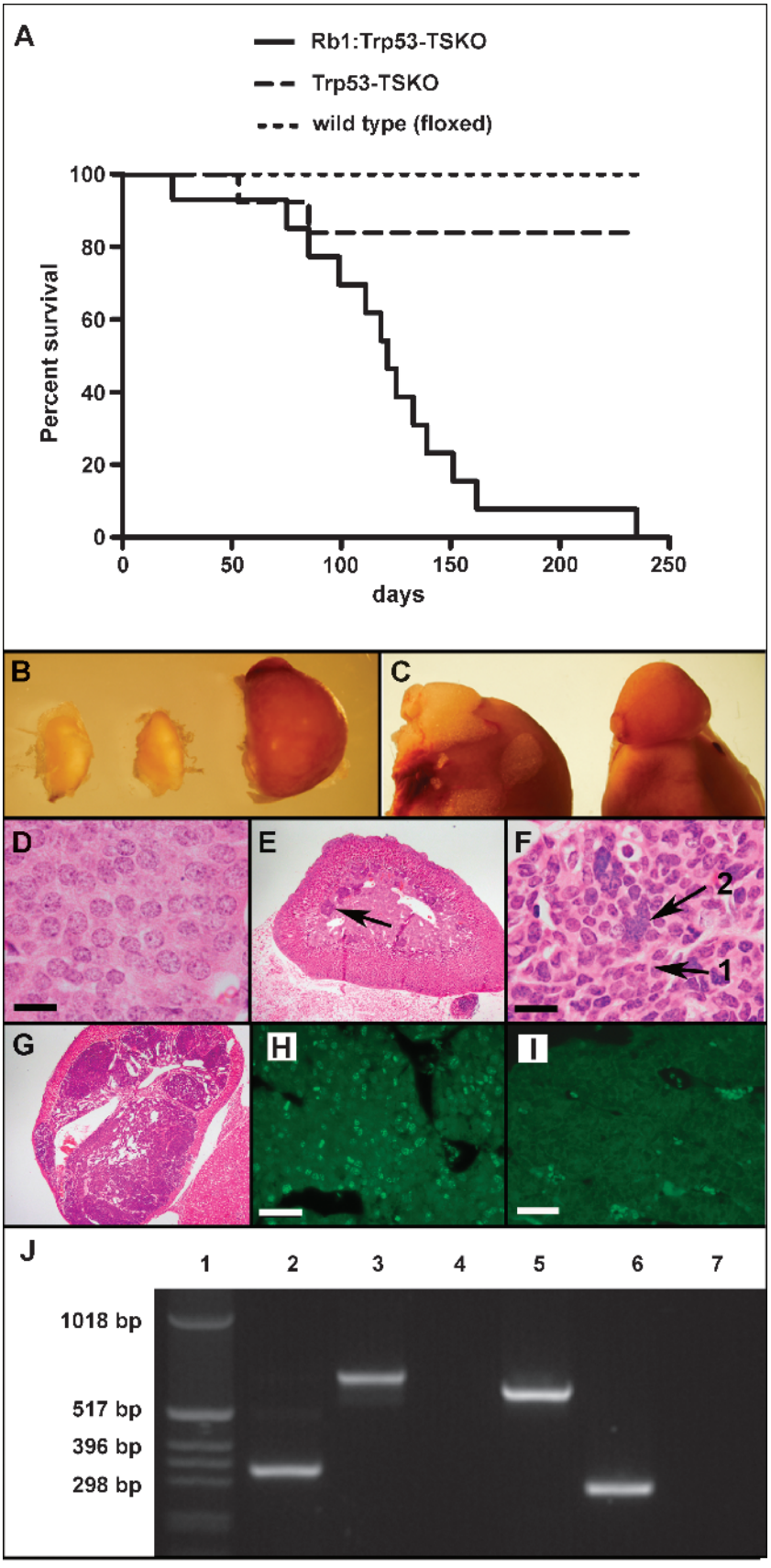
A
Rb1:Trp53-TSKO
Trp53-TSKO
wild type (floxed)
Percent survival
100
80
60
40
20
0
0
50
100
150
200
250
days
B
C
D
E
F
2
1
G
H
I
J
1
2
3
4
5
6
7
1018 bp
517 bp
396 bp
298 bp

to PCR analysis using primers that detect both the floxed and deleted *Rb1* and *Trp53* alleles. The $Rb1^{F2/F2}$:$Trp53^{F2\text{-}10/F2\text{-}10}$:*TEC1* cell line amplified the 329- and 612-bp PCR products corresponding to the deleted *Rb1* (Figure 1*J*, *lane 2*) and *Trp53* alleles (Figure 1*J*, *lane 5*), respectively. No bands corresponding to the product from the floxed allele were apparent, unlike the PCR of chromaffin cell DNA from $Rb1^{F2/F2}$:$Trp53^{F2\text{-}10/F2\text{-}10}$ animals (Figure 1*J*, *lanes 3 and 6*), indicating that the cultured cells had undergone complete Cre-mediated deletion of the floxed *Rb1* and *Trp53* alleles.

In summary, these data show that the loss of *Rb1* and *Trp53* in the adrenal medulla of $Rb1^{F2/F2}$:$Trp53^{F2\text{-}10/F2\text{-}10}$:*TEC1* mice, as driven by Cre expression from the *TEC1* transgene, underpin chromaffin cell hyperplasia and the rapid onset of bilateral PCC with 100% penetrance. To determine whether PCC is responsible for the phenotype of the $Rb1^{F2/F2}$:$Trp53^{F2\text{-}10/F2\text{-}10}$:*TEC1* mice, the adrenal medullas of these animals were subjected to further characterization.

$Rb1^{-/-}$:$Trp53^{-/-}$ Adrenal Chromaffin Cells Actively Synthesize, but May Not Be Able to Appropriately Store, Catecholamines

Because PCCs are typically benign tumors whose negative physiological impact is exerted by paroxysmal hypertensive episodes resulting from inappropriate catecholamine release [31,32], our analysis focused on aspects of chromaffin cell biology pertaining to these issues. The enzymatic systems required for catecholamine synthesis seem to be relatively intact in $Rb1^{-/-}$:$Trp53^{-/-}$ chromaffin cells because the expression of tyrosine hydroxylase, a key enzyme in catecholamine catabolism, was intact in $Rb1^{F2/F2}$:$Trp53^{F2\text{-}10/F2\text{-}10}$ (Figure 2*A*) chromaffin cells and was readily detectable, albeit at slightly reduced levels, in the medullas of $Rb1^{F2/F2}$:$Trp53^{F2\text{-}10/F2\text{-}10}$:*TEC1* (Figure 2*B*) mice. The presence of these enzymatic systems translated into the production of functional bioamines because they could be detected by virtue of the fluorescence generated by the glyoxylic condensation reaction assay when it was performed on sections of unfixed adrenal gland tissue from the $Rb1^{F2/F2}$:$Trp53^{F2\text{-}10/F2\text{-}10}$ (Figure 2*C*), $Rb1^{F2/+}$:$Trp53^{F2\text{-}10/F2\text{-}10}$:*TEC1* (Figure 2*D*), and $Rb1^{F2/F2}$:$Trp53^{F2\text{-}10/F2\text{-}10}$:*TEC1* (Figure 2*E*) mice, compared with controls (Figure 2*F*).

To determine whether the catecholamines were correctly stored, the adrenal medullas of $Rb1^{F2/F2}$:$Trp53^{F2\text{-}10/F2\text{-}10}$ and $Rb1^{F2/F2}$:$Trp53^{F2\text{-}10/F2\text{-}10}$:*TEC1* mice were subjected to immunohistochemistry for chromogranin A and synaptophysin, both components of chromaffin cell secretory vesicles. Unlike the $Rb1^{F2/F2}$:$Trp53^{F2\text{-}10/F2\text{-}10}$ controls (Figure 3, *A* and *C*), the adrenal medullas of $Rb1^{F2/F2}$:$Trp53^{F2\text{-}10/F2\text{-}10}$:*TEC1* mice lacked strong chromogranin A (Figure 3*B*) and synaptophysin (Figure 3*D*) staining, although a somewhat diffuse pattern was

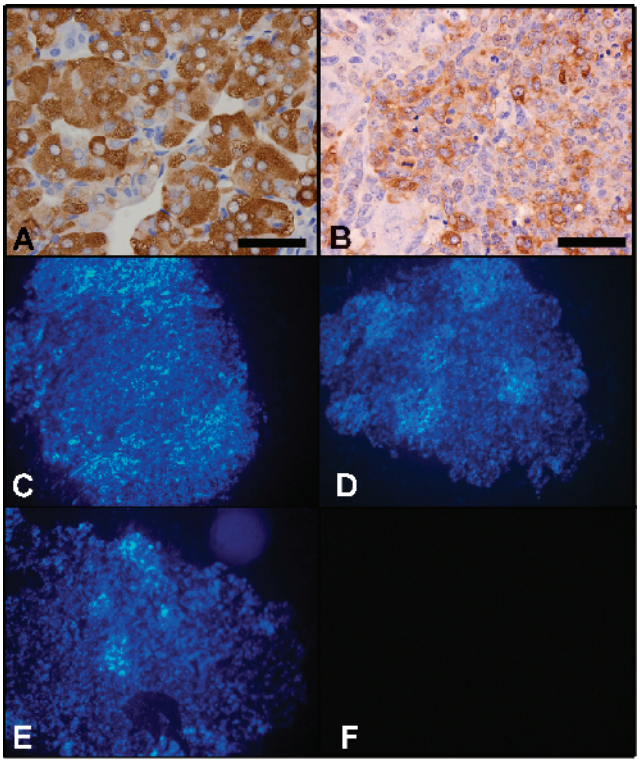

Figure 2. The effect of compound *Rb1* and *Trp53* loss on catecholamine synthesis in the adrenal chromaffin cells. The integrity of catecholamine biosynthetic pathways in $Rb1^{F2/F2}$:$Trp53^{F2\text{-}10/F2\text{-}10}$ (A) and $Rb1^{F2/F2}$:$Trp53^{F2\text{-}10/F2\text{-}10}$:*TEC1* (B) adrenal glands was examined by immunohistochemical detection of tyrosine hydroxylase. Glyoxylic condensation reactions to detect active biogenic amines were performed on the adrenal glands from $Rb1^{F2/F2}$:$Trp53^{F/F}$ (C), $Rb1^{F2/+}$:$Trp53^{F/F}$:*TEC1* (D), and $Rb1^{F2/F2}$:$Trp53^{F/F}$:*TEC1* (E) mice. As a control, the experiment was performed using a serial section from the $Rb1^{F2/F2}$:$Trp53^{F/F}$:*TEC1* adrenal gland, and the glyoxylic acid was omitted from the reaction (F).

Figure 1. The compound loss of *Rb1* and *Trp53* in mouse *Tyr* transcriptional domains profoundly shortens the life span of $Rb1^{F2/F2}$:$Trp53^{F2\text{-}10/F2\text{-}10}$:*TEC1* mice by potentially inducing PCC. A Kaplan-Meier survival curve was constructed for $Rb1^{F2/F2}$:$Trp53^{F2\text{-}10/F2\text{-}10}$:*TEC1* (Rb1:Trp53-TSKO) mice *versus* $Rb1^{F2/+}$:$Trp53^{F2\text{-}10/F2\text{-}10}$:*TEC1* (Trp53-TSKO) and floxed (wild type) control animals. With $n = 13$ in each group, data are shown to be statistically significant ($P < .0001$) with a median survival of double knockouts being 121 days (A). The adrenal glands from 16-week-old $Rb1^{F2/F2}$:$Trp53^{F2\text{-}10/F2\text{-}10}$ (left) and $Rb1^{F2/+}$:$Trp53^{F2\text{-}10/F2\text{-}10}$:*TEC1* (middle) mice are smaller than those of $Rb1^{F2/F2}$:$Trp53^{F2\text{-}10/F2\text{-}10}$:*TEC1* mice (B). For further dimensional perspective, $Rb1^{F2/F2}$:$Trp53^{F2\text{-}10/F2\text{-}10}$ adrenal gland (left) and $Rb1^{F2/F2}$:$Trp53^{F2\text{-}10/F2\text{-}10}$:*TEC1* (right) adrenal glands are shown still attached to the kidneys (C). H&E-stained paraffin sections of chromaffin cells from $Rb1^{F2/F2}$:$Trp53^{F2\text{-}10/F2\text{-}10}$ adrenal medullas showing that they are of very consistent size and shape (D). Scale bar, 50 μm. Histologic analysis of 56 days postpartum $Rb1^{F2/F2}$:$Trp53^{F2\text{-}10/F2\text{-}10}$:*TEC1* adrenal glands shows distinct foci of hyperplastic cells (arrow) (E). Higher magnification of the hyperplastic $Rb1^{F2/F2}$:$Trp53^{F2\text{-}10/F2\text{-}10}$:*TEC1* chromaffin cells showing a lack of uniformity in nuclei size, with both smaller nuclei (black arrow 1) and large polyploid nuclear aggregations apparent (black arrow 2) (F). Scale bar represents 50, 50 μm. By 112 days postpartum, the adrenal medulla was essentially completely occupied by transformed cells and the cortex was compressed (G). Cellular proliferation in $Rb1^{F2/F2}$:$Trp53^{F2\text{-}10/F2\text{-}10}$:*TEC1* (H) and $Rb1^{F2/F2}$:$Trp53^{F2\text{-}10/F2\text{-}10}$ (I) adrenal glands was assessed by Ki67 immunohistochemistry. Scale bar, 200 μm. To determine the status of *Rb1* and *Trp53* alleles in the chromaffin cells derived from $Rb1^{F2/F2}$:$Trp53^{F2\text{-}10/F2\text{-}10}$:*TEC1* mice and those extracted from $Rb1^{F2/F2}$:$Trp53^{F2\text{-}10/F2\text{-}10}$ adrenal glands, they were PCR-genotyped with the Rb5-2/$Rb_{amp2\text{-}2}$/$Rb_{amp3\text{-}2}$ and T008/T009/T011 primer combinations to amplify products from the *Rb1* and *Trp53* alleles, respectively (J). Lane designations are as follows: 1, 1-kb ladder; 2-4, *Rb1* genotyping for $Rb1^{F2/F2}$:$Trp53^{F2\text{-}10/F2\text{-}10}$:*TEC1* (2), $Rb1^{F2/F2}$:$Trp53^{F2\text{-}10/F2\text{-}10}$ (3), and negative control (4); 5-7, *Trp53* genotyping for $Rb1^{F2/F2}$:$Trp53^{F2\text{-}10/F2\text{-}10}$:*TEC1* (5), $Rb1^{F2/F2}$:$Trp53^{F2\text{-}10/F2\text{-}10}$ (6), and negative control (7).

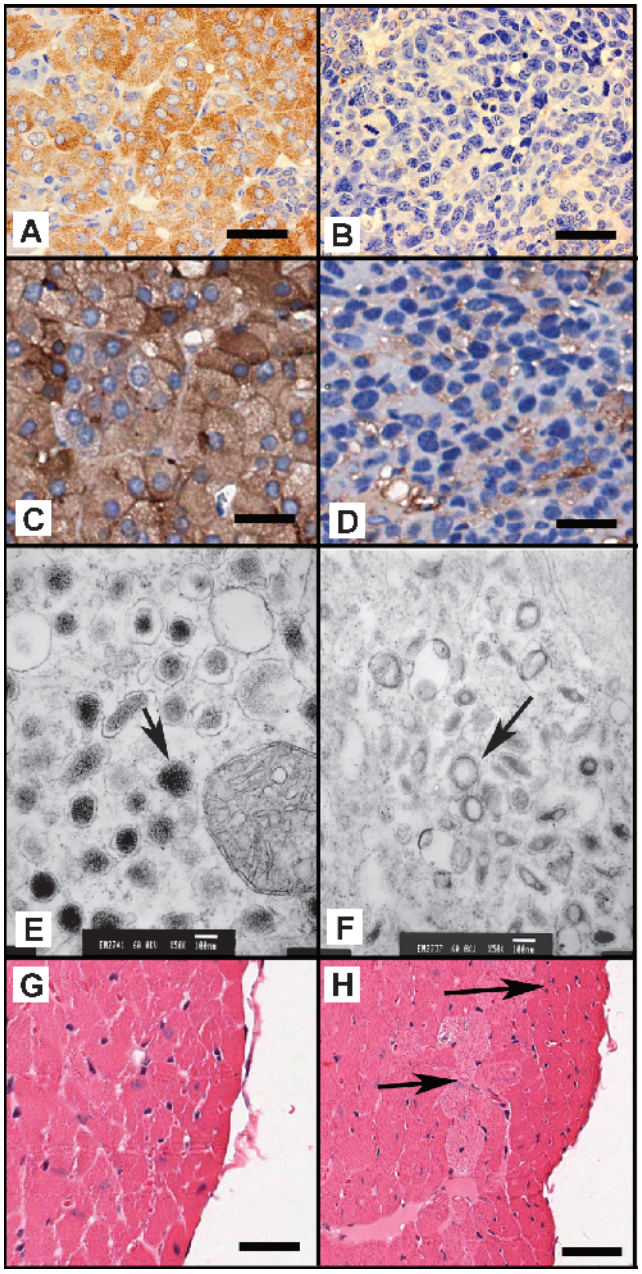

Figure 3. To assess the status of catecholamine storing vesicles, immunohistochemistry was performed for chromogranin A in $Rb1^{F2/F2}$:$Trp53^{F2\text{-}10/F2\text{-}10}$ (A) and $Rb1^{F2/F2}$:$Trp53^{F2\text{-}10/F2\text{-}10}$:*TEC1* (B) and synaptophysin in $Rb1^{F2/F2}$:$Trp53^{F2\text{-}10/F2\text{-}10}$ (C) and $Rb1^{F2/F2}$:$Trp53^{F2\text{-}10/F2\text{-}10}$:*TEC1* (D) adrenal medullas. Scale bar, 50 μm. Electron micrographs of $Rb1^{F2/F2}$:$Trp53^{F/F}$ (E; original magnification, ×50,000) and $Rb1^{F2/F2}$:$Trp53^{F/F}$:*TEC1* (F; original magnification, ×50,000) chromaffin cells showing the overall density and morphology of vesicles (arrow). H&E staining of $Rb1^{F2/F2}$:$Trp53^{F2\text{-}10/F2\text{-}10}$ (G) and $Rb1^{F2/F2}$:$Trp53^{F2\text{-}10/F2\text{-}10}$:*TEC1* (H) heart sections that shows structural remodeling of the $Rb1^{F2/F2}$:$Trp53^{F2\text{-}10/F2\text{-}10}$:*TEC1* hearts (as indicated by arrows).

obtained in each case. To confirm this result and ascertain whether compromised synaptophysin expression was common in $Rb1^{-/-}$:$Trp53^{-/-}$ chromaffin cells, further adrenal glands from $Rb1^{F2/F2}$:$Trp53^{F2\text{-}10/F2\text{-}10}$:*TEC1* mice ($n$ = 5) were subjected to synaptophysin immunohistochemistry. The expression levels of synaptophysin seemed to be highly variable between both PCCs and even within a given sample. However, whereas synaptophysin always seemed present, it was generally at much lower levels than in normal adrenal medullas (data not shown).

To more closely examine the ultrastructure of $Rb1^{-/-}$:$Trp53^{-/-}$ chromaffin cells, with a specific emphasis on chromagenic vesicles, they were subjected to electron microscopy. The control $Rb1^{F2/F2}$:$Trp53^{F/F}$ chromaffin cells possessed a high concentration of electron dense chromagenic granules (Figure 3*E*). In contrast, the $Rb1^{F2/F2}$:$Trp53^{F/F}$:*TEC1* chromaffin cells had smaller vesicles, but these adopted an almost halo-like appearance and lacked any electron dense material (Figure 3*F*). These data show that whereas the $Rb1^{F2/F2}$:$Trp53^{F/F}$:*TEC1* chromaffin cells have vesicles typical of pheochromocytes, their functional integrity may be compromised, as indicated by the chromogranin A and synaptophysin immunohistochemistry, so they do not store catecholamines at a capacity or in a way typical of normal chromaffin cells.

The inappropriate catecholamine release deriving from PCC can have profound structural effects on the heart [31,32]. Consequently, hearts were taken from 3.5-month-old $Rb1^{F2/F2}$:$Trp53^{F/F}$:*TEC1* and $Rb1^{F2/F2}$:$Trp53^{F/F}$ mice (n = 3 for each genotype), sectioned and examined for obvious defects. In contrast to the hearts from $Rb1^{F2/F2}$:$Trp53^{F/F}$, which all appeared normal (Figure 3*G*), structural remodeling of the left ventricle was apparent in all $Rb1^{F2/F2}$:$Trp53^{F/F}$:*TEC1* hearts (Figure 3*H*). Because the heart does not express the Cre transgene, these secondary changes may be PCC-derived. Overall, the phenotype described for the $Rb1^{F2/F2}$:$Trp53^{F2\text{-}10/F2\text{-}10}$:$TEC1^{+/-}$ mice is consistent with that expected for PCC because it indicates that they may succumb to the catecholamine-induced effects of benign PCC, highlighting the important role that the *Rb1* and *Trp53* tumor suppressor genes fulfill in chromaffin cell homeostasis.

Discussion

PCC is a relatively rare and typically benign tumor type [33,34]. Despite this, they are clinically significant because their overproduction of catecholamine can result in potentially lethal paroxysmal or sustained hypertensive episodes [31,32].

Insights into the genetic basis and molecular mechanisms that govern the maintenance of chromaffin cell homeostasis have been provided by the identification of genes mutated in familial PCC syndromes, which include *NF1*, *RET*, *VHL*, or *SDH* [35]. PCCs are also observed when general tumor suppressor genes, such as *p18* and *Pten*, are mutated. Mice mutant for *p18* and *Pten* develop PCC at frequencies of 14% and 65%, respectively [36], but the percentage can be significantly heightened when *p18* and *Pten* are either comutated or mutated in combination with other tumor suppressor genes (e.g., $p18^{-/-}$:$p27^{-/-}$, $p18^{-/-}$:$Pten^{+/-}$, $p27^{-/-}$:$Pten^{-/-}$, and $Pten^{+/-}$:$Ink4a/arf^{+/-}$ compound mutant mice develop PCC at frequencies of 91% [6], 84% [36], 100% [37], and 81% [7], respectively). This indicates that a significant degree of synergism exists between these tumor suppressive pathways in maintaining chromaffin cell homeostasis.

A common point of action of these genes is their ability to modulate Cdk-cyclin function (as reviewed in Tonks et al. [14]). Indicating that loss of normally stringent Cdk-cyclin regulation at multiple points in the cell cycle of chromaffin cells may be an important factor for PCC development. The primary targets of Cdk-cyclin function in cell cycle regulation are the PPs, indicating that they may have a key role in chromaffin cell homeostasis. Indeed, the perturbation of PP function may also be integral to the manifestation of familial PCC

syndromes as the mutation of *RET*, *NF1*, or *VHL* contribute to increased Cdk-cyclin function and decreased PP function by a number of mechanisms, such as decreased CKI levels, increased cyclin and Cdk expression, or decreased expression of other Cdk-cyclin inhibitors, for example, 14-3-3-epsilon [38–45].

Because Rb1 is known to have the most significant tumor suppressive function of the PP family, it is likely that its functional integrity is integral to adrenal chromaffin cell homeostasis. Indeed, support for this theory comes from the phenotype of $Rb1^{-/-}$:$Rb1^{+/+}$ chimeric mice, where 67% developed hyperplastic nodules of the adrenal medulla before succumbing to pituitary gland tumors at 6 months [19,46]. Further, a study of $Rb1^{+/-}$ mouse cohorts by Nikitin et al. [18] indicated that 71% of $Rb^{+/-}$ heterozygous mice developed PCC, with 14% of those being bilateral. It must be noted, however, that the lesions classified as PCC included those that appear as small foci of atypical cells. Consequently, Nikitin et al. [18] may be overestimating the frequency of PCC; as such, lesions would usually be classified as chromaffin cell hyperplasia [20]. Significantly, however, the hyperplastic cells noted early in the course of the disease had loss of heterozygosity for the remaining wild-type *Rb1* allele, supporting the findings from $Rb1^{-/-}$:$Rb1^{+/+}$ chimeras. Furthermore, data derived from human PCC show that, despite *Rb1* loss being relatively common, there is no significant difference between *Rb1*-positive and -negative PCCs in malignant potential and survival of patients [21]. This indicates that the rate of conversion from chromaffin cell hyperplasia to PCC driven by *Rb1* loss can be enhanced by the mutation of other genetic modifiers.

Other PPs are obvious candidate tumor suppressor genes that may interact with *Rb1* in the progression of PCC. Indeed, the loss of *Rbl2*, but not *Rbl1*, can exacerbate the development and decrease the latency of PCC development occurring in *Rb1*-deficient mouse models [13]. We have now shown that *Trp53*, another gene involved in maintaining genomic integrity, can also synergize with *Rb1* loss in the development of PCC. This was obvious *in vitro*, as $Rb1^{-/-}$:$Trp53^{-/-}$ chromaffin cells were readily established in culture, whereas $Rb1^{-/-}$ or $Trp53^{-/-}$ cells could not be cultured under the same conditions. Concordantly, the *in vivo* compound loss of these two genes had a profound effect, yielding bilateral PCCs in all $Rb1^{F2/F2}$:$Trp53^{F/F}$:*TEC1* individuals examined to date.

Whereas *Rb1* loss is important at the level of cellular proliferation and hyperplasia during the initial stages of PCC development, the role of Trp53 has been controversial. For example, *Trp53* mutation has been identified in PCC [21], but a recent study by Petri et al. [47] of benign and malignant PCC using CGH coupled to immunohistochemistry showed that Trp53 function does not contribute significantly to the development of PCC. In our study, $Rb1^{F/+}$:$Trp53^{F/F}$:*TEC1* mice, like $Rb1^{+/-}$:$Trp53^{-/}$ and $Trp53^{-/-}$ mice described elsewhere [48,49], did not get PCC at any substantial frequency, but the $Rb1^{F2/F2}$:$Trp53^{F2\text{-}10/F2\text{-}10}$:*TEC1* cohort succumbed to the disease with complete penetrance. Consequently, *Trp53* is significant to PCC development, but only when this occurs on a background of predisposing mutations, such as *Rb1*.

There are a number of potential mechanisms by which *Trp53* mutation may act synergistically with *Rb1* loss in the development of PCC. In the first, the Trp53/Arf/Mdm2 regulatory axis can exert a direct effect on the overall PP function (reviewed in Tonks et al. [14]). Consequently, compound loss of *Rb1* and *Trp53* functions in the development of PCC may be similar to that caused by *Rb1* and *Rbl2*.

In the second instance, recent work has suggested that *Trp53* loss may act to fundamentally change the metabolism of tumor cells to expedite neoplastic transformation. Tumor cells use anaerobic glycolysis as a primary metabolic pathway, even under normal aerobic conditions, and this phenomenon, known as the Warburg effect, confers a proliferative advantage to the mutated cells by allowing the increased synthesis of biomolecules integral to proliferation [50]. The Warburg effect may be enhanced in *Trp53*-null cells by a number of mechanisms.

First, *Trp53* loss in VHL-related (familial) PCC may lead to a hypoxic growth response through promiscuous hypoxia-inducible factor activation in tumor cells, so that they primarily use glycolysis as their energy source [51]. This potentially reconciles our results on *Trp53* with familial PCC because VHL is known to bind Trp53 and protect it from degradation. This may not just appropriately maintain aerobic respiration but, in response to genotoxic stress, it potentiates Trp53-mediated transcriptional activity, cell cycle arrest, and apoptosis, all of which are integral to cellular homeostasis [51,52].

Second, *Trp53*-loss may inhibit the expression of key genes involved in aerobic respiration, such as Sco2 and TIGAR. *Sco2* is the cytochrome *c* oxidase assembly factor necessary for oxygen consumption and the activity of the oxidative phosphorylation IV complex [53], whereas TIGAR expression acts to downregulate glycolysis, and they could act in a concerted manner to inhibit the Warburg effect [54]. Third, the loss of Trp53 can also cause depletion of mitochondrial DNA and associated mitochondrial mass, presumably leading to reduced mitochondrial oxidative capacity [55].

Collectively, this suggests that *Trp53* mutation may potentially exacerbate PCC development in $Rb1^{F2/F2}$:$Trp53^{F2\text{-}10/F2\text{-}10}$:*TEC1* mice at a number of levels, including decreased PP function by a number of mechanisms as well as by establishing a metabolic environment permissible to the Warburg effect and tumor growth.

Despite the apparent proliferative capacity of $Rb1^{-/-}$:$Trp53^{-/-}$ chromaffin cells, the resultant PCCs are generally benign and do not metastasize. Nonetheless, they seem to manifest a profound effect on mouse physiology, presumably at the cardiac level, which seems to result from the inability of the PCCs to appropriately store the catecholamines that they synthesize. Ultimately, this shows that the synergistic effects of *Rb1* and *Trp53* are essential in maintaining both adrenal chromaffin cell homeostasis and animal vitality.

Acknowledgment

The authors thank Clay Winterford for his assistance with the tissue sectioning and electron microscopy.

References

[1] Cheng M, Olivier P, Diehl JA, Fero M, Roussel MF, Roberts JM, and Sherr CJ (1999). The p21(Cip1) and p27(Kip1) CDK "inhibitors" are essential activators of cyclin D–dependent kinases in murine fibroblasts. *EMBO J* **18**, 1571–1583.

[2] Sherr CJ and Roberts JM (1999). CDK inhibitors: positive and negative regulators of G_1-phase progression. *Genes Dev* **13**, 1501–1512.

[3] Jiang H, Chou HS, and Zhu L (1998). Requirement of cyclin E–Cdk2 inhibition in p16(INK4a)-mediated growth suppression. *Mol Cell Biol* **18**, 5284–5290.

[4] Gius DR, Ezhevsky SA, Becker-Hapak M, Nagahara H, Wei MC, and Dowdy SF (1999). Transduced $p16^{INK4a}$ peptides inhibit hypophosphorylation of the retinoblastoma protein and cell cycle progression prior to activation of Cdk2 complexes in late G_1. *Cancer Res* **59**, 2577–2580.

[5] Kiss NB, Geli J, Lundberg F, Avci C, Velazquez-Fernandez D, Hashemi J, Weber G, Hoog A, Ekstrom TJ, Backdahl M, et al. (2008). Methylation of the $p16^{INK4A}$ promoter is associated with malignant behavior in abdominal extra-adrenal paragangliomas but not pheochromocytomas. *Endocr Relat Cancer* **15**, 609–621.

[6] Franklin DS, Godfrey VL, O'Brien DA, Deng C, and Xiong Y (2000). Functional collaboration between different cyclin-dependent kinase inhibitors suppresses tumor growth with distinct tissue specificity. *Mol Cell Biol* **20**, 6147–6158.

[7] You MJ, Castrillon DH, Bastian BC, O'Hagan RC, Bosenberg MW, Parsons R, Chin L, and DePinho RA (2002). Genetic analysis of Pten and Ink4a/Arf interactions in the suppression of tumorigenesis in mice. *Proc Natl Acad Sci USA* **99**, 1455–1460.

[8] Schraml P, Bucher C, Bissig H, Nocito A, Haas P, Wilber K, Seelig S, Kononen J, Mihatsch MJ, Dirnhofer S, et al. (2003). Cyclin E overexpression and amplification in human tumours. *J Pathol* **200**, 375–382.

[9] Helin K, Holm K, Niebuhr A, Eiberg H, Tommerup N, Hougaard S, Poulsen HS, Spang-Thomsen M, and Norgaard P (1997). Loss of the retinoblastoma protein–related p130 protein in small cell lung carcinoma. *Proc Natl Acad Sci USA* **94**, 6933–6938.

[10] Cinti C, Claudio PP, Howard CM, Neri LM, Fu Y, Leoncini L, Tosi GM, Maraldi NM, and Giordano A (2000). Genetic alterations disrupting the nuclear localization of the retinoblastoma-related gene RB2/p130 in human tumor cell lines and primary tumors. *Cancer Res* **60**, 383–389.

[11] Claudio PP, Howard CM, Pacilio C, Cinti C, Romano G, Minimo C, Maraldi NM, Minna JD, Gelbert L, Leoncini L, et al. (2000). Mutations in the retinoblastoma-related gene RB2/p130 in lung tumors and suppression of tumor growth *in vivo* by retrovirus-mediated gene transfer. *Cancer Res* **60**, 372–382.

[12] Robanus-Maandag E, Dekker M, van der Valk M, Carrozza ML, Jeanny JC, Dannenberg JH, Berns A, and te Riele H (1998). p107 is a suppressor of retinoblastoma development in pRb-deficient mice. *Genes Dev* **12**, 1599–1609.

[13] Dannenberg JH, Schuijff L, Dekker M, van der Valk M, and Riele HT (2004). Tissue-specific tumor suppressor activity of retinoblastoma gene homologs p107 and p130. *Genes Dev* **18**, 2952–2962.

[14] Tonks ID, Hayward NK, and Kay GF (2006). Pocket protein function in melanocyte homeostasis and neoplasia. *Pigment Cell Res* **19**, 260–283.

[15] Classon M, Kennedy BK, Mulloy R, and Harlow E (2000). Opposing roles of pRB and p107 in adipocyte differentiation. *Proc Natl Acad Sci USA* **97**, 10826–10831.

[16] Carnac G, Fajas L, L'Honore A, Sardet C, Lamb NJ, and Fernandez A (2000). The retinoblastoma-like protein p130 is involved in the determination of reserve cells in differentiating myoblasts. *Curr Biol* **10**, 543–546.

[17] MacPherson D, Sage J, Crowley D, Trumpp A, Bronson RT, and Jacks T (2003). Conditional mutation of Rb causes cell cycle defects without apoptosis in the central nervous system. *Mol Cell Biol* **23**, 1044–1053.

[18] Nikitin AY, Juarez-Perez MI, Li S, Huang L, and Lee WH (1999). RB-mediated suppression of spontaneous multiple neuroendocrine neoplasia and lung metastases in Rb+/– mice. *Proc Natl Acad Sci USA* **96**, 3916–3921.

[19] Williams BO, Schmitt EM, Remington L, Bronson RT, Albert DM, Weinberg RA, and Jacks T (1994). Extensive contribution of Rb-deficient cells to adult chimeric mice with limited histopathological consequences. *EMBO J* **13**, 4251–4259.

[20] Longeart LE (1996).Jones TC, Capen CC, and Mohr U (1996). Adrenal medullary tumours, mouse. *Monographs on Pathology of Laboratory Animals. Endocrine System* Berlin, Germany: Springer-Verlag, 421–427.

[21] Lam KY, Lo CY, Wat NM, Luk JM, and Lam KS (2001). The clinicopathological features and importance of p53, Rb, and mdm2 expression in phaeochromocytomas and paragangliomas. *J Clin Pathol* **54**, 443–448.

[22] Dannenberg JH, Schuijff L, Dekker M, van der Valk M, and te Riele H (2004). Tissue-specific tumor suppressor activity of retinoblastoma gene homologs p107 and p130. *Genes Dev* **18**, 2952–2962.

[23] Tonks ID, Hacker E, Irwin N, Muller HK, Keith P, Mould A, Zournazi A, Pavey S, Hayward NK, Walker G, et al. (2005). Melanocytes in conditional $Rb^{-/-}$ mice are normal *in vivo* but exhibit proliferation and pigmentation defects *in vitro*. *Pigment Cell Res* **18**, 252–264.

[24] Tonks ID, Nurcombe V, Paterson C, Zournazi A, Prather C, Mould AW, and Kay GF (2003). Tyrosinase-Cre mice for tissue-specific gene ablation in neural crest and neuroepithelial-derived tissues. *Genesis* **37**, 131–138.

[25] Jonkers J, Meuwissen R, van der Gulden H, Peterse H, van der Valk M, and Berns A (2001). Synergistic tumor suppressor activity of BRCA2 and p53 in a conditional mouse model for breast cancer. *Nat Genet* **29**, 418–425.

[26] Walker GJ, Kimlin MG, Hacker E, Ravishankar S, Muller HK, Beermann F, and Hayward NK (2009). Murine neonatal melanocytes exhibit a heightened proliferative response to ultraviolet radiation and migrate to the epidermal basal layer. *J Invest Dermatol* **129**, 184–193.

[27] Allan DJ, Gobe GC, and Harmon BV (1988). Sertoli cell death by apoptosis in the immature rat testis following x-irradiation. *Scanning Microsc* **2**, 503–512.

[28] De la Torre JC (1980). An improved approach to histofluorescence using the SPG method for tissue monoamines. *J Neurosci Methods* **3**, 1–5.

[29] Tonks ID, Mould A, Nurcombe V, Cool SM, Walker GJ, Hacker E, Keith P, Schroder WA, Cotterill A, Hayward NK, et al. (2009). Dual loss of Rb1 and Trp53 in melanocytes perturbs melanocyte homeostasis and genetic stability *in vitro* but does not cause melanoma or pigmentation defects *in vivo*. *Pigment Cell Melanoma Res* **22**, 328–330.

[30] Jones GN, Tep C, Towns WH II, Mihai G, Tonks ID, Kay GF, Schmalbrock PM, Stemmer-Rachamimov AO, Yoon SO, and Kirschner LS (2008). Tissue-specific ablation of Prkar1a causes schwannomas by suppressing neurofibromatosis protein production. *Neoplasia* **10**, 1213–1221.

[31] Hoffman BB (1991). Adrenergic pharmacology in rats harboring pheochromocytoma. *Hypertension* **18**, III35–III39.

[32] Gimm O (2005). Pheochromocytoma-associated syndromes: genes, proteins and functions of RET, VHL and SDHx. *Fam Cancer* **4**, 17–23.

[33] Melicow MM (1977). One hundred cases of pheochromocytoma (107 tumors) at the Columbia-Presbyterian Medical Center, 1926-1976: a clinicopathological analysis. *Cancer* **40**, 1987–2004.

[34] Proye C, Vix M, Goropoulos A, Kerlo P, and Lecomte-Houcke M (1992). High incidence of malignant pheochromocytoma in a surgical unit. 26 cases out of 100 patients operated from 1971 to 1991. *J Endocrinol Invest* **15**, 651–663.

[35] Mannelli M, Simi L, Gagliano MS, Opocher G, Ercolino T, Becherini L, and Parenti G (2007). Genetics and biology of pheochromocytoma. *Exp Clin Endocrinol Diabetes* **115**, 160–165.

[36] Bai F, Pei XH, Pandolfi PP, and Xiong Y (2006). p18 Ink4c and Pten constrain a positive regulatory loop between cell growth and cell cycle control. *Mol Cell Biol* **26**, 4564–4576.

[37] Di Cristofano A, De Acetis M, Koff A, Cordon-Cardo C, and Pandolfi PP (2001). Pten and $p27^{KIP1}$ cooperate in prostate cancer tumor suppression in the mouse. *Nat Genet* **27**, 222–224.

[38] Joshi PP, Kulkarni MV, Yu BK, Smith KR, Norton DL, Veelen W, Hoppener JW, and Franklin DS (2007). Simultaneous downregulation of CDK inhibitors p18(Ink4c) and p27(Kip1) is required for MEN2A-RET–mediated mitogenesis. *Oncogene* **26**, 554–570.

[39] Basu TN, Gutmann DH, Fletcher JA, Glover TW, Collins FS, and Downward J (1992). Aberrant regulation of ras proteins in malignant tumour cells from type 1 neurofibromatosis patients. *Nature* **356**, 713–715.

[40] Bollag G, Clapp DW, Shih S, Adler F, Zhang YY, Thompson P, Lange BJ, Freedman MH, McCormick F, Jacks T, et al. (1996). Loss of NF1 results in activation of the Ras signaling pathway and leads to aberrant growth in haematopoietic cells. *Nat Genet* **12**, 144–148.

[41] DeClue JE, Papageorge AG, Fletcher JA, Diehl SR, Ratner N, Vass WC, and Lowy DR (1992). Abnormal regulation of mammalian $p21^{ras}$ contributes to malignant tumor growth in von Recklinghausen (type 1) neurofibromatosis. *Cell* **69**, 265–273.

[42] Kim HA, Ratner N, Roberts TM, and Stiles CD (2001). Schwann cell proliferative responses to cAMP and Nf1 are mediated by cyclin D1. *J Neurosci* **21**, 1110–1116.

[43] Kim HA, Rosenbaum T, Marchionni MA, Ratner N, and DeClue JE (1995). Schwann cells from neurofibromin deficient mice exhibit activation of $p21^{ras}$, inhibition of cell proliferation and morphological changes. *Oncogene* **11**, 325–335.

[44] Zatyka M, da Silva NF, Clifford SC, Morris MR, Wiesener MS, Eckardt KU, Houlston RS, Richards FM, Latif F, and Maher ER (2002). Identification of cyclin D1 and other novel targets for the von Hippel–Lindau tumor suppressor gene by expression array analysis and investigation of cyclin D1 genotype as a modifier in von Hippel–Lindau disease. *Cancer Res* **62**, 3803–3811.

[45] Wykoff CC, Sotiriou C, Cockman ME, Ratcliffe PJ, Maxwell P, Liu E, and Harris AL (2004). Gene array of VHL mutation and hypoxia shows novel hypoxia-induced genes and that cyclin D1 is a VHL target gene. *Br J Cancer* **90**, 1235–1243.

[46] Maandag EC, van der Valk M, Vlaar M, Feltkamp C, O'Brien J, van Roon M, van der Lugt N, Berns A, and te Riele H (1994). Developmental rescue of an embryonic-lethal mutation in the retinoblastoma gene in chimeric mice. *EMBO J* **13**, 4260–4268.

[47] Petri BJ, Speel EJ, Korpershoek E, Claessen SM, van Nederveen FH, Giesen V, Dannenberg H, van der Harst E, Dinjens WN, and de Krijger RR (2008). Frequent loss of 17p, but no p53 mutations or protein overexpression in benign and malignant pheochromocytomas. *Mod Pathol* **21**, 407–413.

[48] Williams BO, Remington L, Albert DM, Mukai S, Bronson RT, and Jacks T (1994). Cooperative tumorigenic effects of germline mutations in Rb and p53. *Nat Genet* **7**, 480–484.

[49] Jacks T, Remington L, Williams BO, Schmitt EM, Halachmi S, Bronson RT, and Weinberg RA (1994). Tumor spectrum analysis in p53-mutant mice. *Curr Biol* **4**, 1–7.

[50] Vander Heiden MG, Cantley LC, and Thompson CB (2009). Understanding the Warburg effect: the metabolic requirements of cell proliferation. *Science* **324**, 1029–1033.

[51] Favier J, Briere JJ, Burnichon N, Riviere J, Vescovo L, Benit P, Giscos-Douriez I, De Reynies A, Bertherat J, Badoual C, et al. (2009). The Warburg effect is genetically determined in inherited pheochromocytomas. *PLoS One* **4**, e7094.

[52] Roe JS and Youn HD (2006). The positive regulation of p53 by the tumor suppressor VHL. *Cell Cycle* **5**, 2054–2056.

[53] Matoba S, Kang JG, Patino WD, Wragg A, Boehm M, Gavrilova O, Hurley PJ, Bunz F, and Hwang PM (2006). p53 regulates mitochondrial respiration. *Science* **312**, 1650–1653.

[54] Bensaad K, Tsuruta A, Selak MA, Vidal MN, Nakano K, Bartrons R, Gottlieb E, and Vousden KH (2006). TIGAR, a p53-inducible regulator of glycolysis and apoptosis. *Cell* **126**, 107–120.

[55] Lebedeva MA, Eaton JS, and Shadel GS (2009). Loss of p53 causes mitochondrial DNA depletion and altered mitochondrial reactive oxygen species homeostasis. *Biochim Biophys Acta* **1787**, 328–334.